Optik 127 (2016) 1962–1966

Contents lists available at ScienceDirect

Optik

journal homepage: www.elsevier.de/ijleo

Solvothermal preparation and characterization of ternary alloy CdS_xSe_{1-x} nanowires

M.A. Mahdi [a,*], A. Hmood [b], A. Kadhim [b], J.J. Hassan [a], S.J. Kasim [a], Z. Hassan [c]

[a] Basrah Nanomaterials Research Group (BNRG), Physics Department, College of Science, Basrah University, Basrah, Iraq
[b] Physics Department, College of Science, Basrah University, Basrah, Iraq
[c] Nano-Optoelectronics Research and Technology Laboratory (N.O.R.), School of Physics, University Sains Malaysia, Penang 11800, Malaysia

ARTICLE INFO

Article history:
Received 7 March 2015
Accepted 2 November 2015

Keywords:
Chalcogenides
Chemical synthesis
CdS_xSe_{1-x} nanowires
Nanoparticles

ABSTRACT

CdS_xSe_{1-x} nanowires (NWs) were prepared via solvothermal method. Cadmium chloride ($CdCl_2$), sulfur (S), and selenium (Se) powders were used as Cd^{2+}, S^{2-}, and Se^{2-} ion sources, with ethylenediamine as solvent. The preparation temperature was 200 °C, and the total time was 5 h. The field emission scanning electron microscopy images showed that the CdS_xSe_{1-x} NWs had a uniform shape with diameters varying from 20 nm to 50 nm. The composition ratio (x) of the prepared CdS_xSe_{1-x} was 0.66. The phase composition of the CdS_xSe_{1-x} NWs was characterized by high-resolution X-ray diffraction, which revealed a hexagonal structure. The particle size was found to be approximately 15 nm. The value of the optical band gap was estimated as 2.38 eV. The photoluminescence spectra of the CdS_xSe_{1-x} NWs showed main emission band located at 555 nm (2.23 eV), and two weak broad emission bands were also detected at wavelengths of 826 (1.50 eV) and 880 nm (1.41 eV).

1. Introduction

The synthesis of 1D nanowires (NWs) and the studies of their particular physical properties have attracted much attention on an important class of materials with potential for use in the fabrication and manufacture of next-generation nano/microdevices [1–3]. The control over nanocrystalline morphology and crystal size is an important goal for synthetic chemists and materials scientists [4,5]. Cadmium sulfide (CdS) and cadmium selenide (CdSe) are two very important wide-gap semiconductors because of their wide application in optoelectronics, such as in nonlinear optics, visible light-emitting diodes, and lasers. The alloy CdS_xSe_{1-x} has more applications because its band gap can be tuned by the composition between $E_g = (2.43–2.52)$ eV in CdS and (1.72–1.8) eV in CdSe [6–10]. Thus, the preparation of CdS_xSe_{1-x} alloy is interesting from the band-gap engineering and optoelectronic point of view because this material could cover the entire visible region of the electromagnetic spectrum [11]. The synthesis and color-tunable photoluminescence (PL) of alloyed CdS–CdSe ternary nanostructures have been reported in previous years [12–14]. The luminescence band can be adjusted in the visible wavelength range by changing their constituent stoichiometries. An important feature of alloyed semiconductor NWs is their freedom in band-gap engineering. The large variety of band gaps of these materials leads to a wide spectral response ranging from green to near-infrared [15]. However, nanocrystal materials, such as CdS, CdSe, CdSSe, ZnSe, and Bi_2S_3, are generally synthesized via a variety of techniques, including chemical bath deposition [16,17], thermal evaporation [18–21], solvothermal route [22], sputtering [23], chemical spray pyrolysis [13,15], and melt quenching technique [24]. In the present work, an attempt was made to prepare CdS_xSe_{1-x} NWs via a simple and low-cost solvothermal technique. The surface morphology, crystalline structure, and optical properties of the prepared NWs were studied, and the results were discussed.

2. Experimental

Cadmium chloride ($CdCl_2$), sulfur (S), and selenium (Se) powders were used as Cd^{2+}, S^{2-}, and Se^{2-} ion sources, respectively. Approximately 1.0 g of $CdCl_2$ and 0.25 g each of S and Se powders were dissolved separately in ethylenediamine (en) with continuous stirring for 1 h at room temperature. The solution was poured into a 100 mL Teflon-lined stainless steel autoclave filled with en up to 80% total volume capacity, sealed, and then loaded into an oven. The preparation temperature was 200 °C, and the total time was 5 h. Finally, the autoclave was removed from the oven and allowed to cool naturally. The color of the product was brown-red. The

* Corresponding author. Tel.: +964 0778686096.
E-mail address: mazinauny74@yahoo.com (M.A. Mahdi).

http://dx.doi.org/10.1016/j.ijleo.2015.11.021
0030-4026/

resulting powder was filtered and washed several times in a centrifuge with absolute ethanol and distilled water. The product was then air dried at 50 °C for 2 h. The synthesized CdS_xSe_{1-x} NWs were confirmed by high resolution X-ray diffraction (HXRD) with $CuK_{\alpha 1}$ radiation in the 2θ range of 20°–70°. The surface morphology and composition ratio of the prepared CdS_xSe_{1-x} NWs were determined using FESEM and EDX (FEI Nova NanoSEM 450) with 3.0 kV operating voltage. The transmittance spectrum of the grown CdS_xSe_{1-x} NWs was recorded using a UV–vis double-beam spectrophotometer (model UV-1800) with a wavelength range of 350–900 nm at room temperature. PL and Raman spectra measurements were carried out by exciting with a He–Cd laser light, which was focused on the sample through a spherical lens by using Jobine Yvon HR 800 UV system at excitation wavelengths of 325 and 514 nm, respectively.

3. Results and discussion

3.1. Surface morphology

Fig. 1 shows the high-resolution FESEM micrographs of the grown CdS_xSe_{1-x} NWs. The synthesized CdS_xSe_{1-x} NWs had uniform crystallite sizes and crisscrossed nanostructures with diameters varying from 20 nm to 50 nm. However, in the solvothermal method, the solvent has an important function in nanoparticle fabrication. Ethylenediamine ($H_2NCH_2CH_2NH_2$) solvent is widely used to control the nucleation and growth of NW structure [25]. Cadmium ions (Cd^{2+}) interact with the lone pair electrons of the en nitrogen atoms to form Cd–en $[Cd(en)_2]c^{2+}$, which then reacts with the S^{2-} and Se^{2-} ions in the solution to synthesize CdS_xSe_{1-x} NWs, as shown in the following reaction:

$$Cd - en[Cd(en)_2]^{2+} + xS^{2-} + (1-x)Se^{2-} \rightarrow CdS_xSe_{1-x}0.5(en) \rightarrow CdS_xSe_{1-x} + en \quad (1)$$

The CdS_xSe_{1-x} 0.5 (en) is an organic–inorganic lamellar structure with inorganic CdS_xSe_{1-x} sheets spaced by organic en molecules. This structure could be formed at low formation temperature (≈120 °C), and when the temperature increases to approximately 200 °C, the sheets become unstable and are destroyed into nano-needle structure to achieve stability. The needle-like structure then grows to form nanowires because of the high surface energy. This formation mechanism was suggested by Kar et al. [26] and Wang et al. [27] for CdS nanowires prepared via solvothermal method and proven by Mahdi et al. [25]. However, some grains also showed in the FESEM image possibly because several Cd^{2+} ions did not bond with en; thus, the Cd^{2+} ions reacted with S^{2-} and Se^{2-} ions to form CdS_xSe_{1-x} particles without solvent control according to the reaction:

$$CdCl_2 + xS + (1-x)Se \rightarrow CdS_xSe_{1-x} + 2Cl_2 \quad (2)$$

The elemental composition ratio of the prepared CdS_xSe_{1-x} NWs was determined with EDX analysis as shown Fig. 3. The EDX analysis confirmed the presence of Cd, S, and Se in the CdS_xSe_{1-x} sample with 51.01%, 32.3%, and 16.69%, respectively. Thus, the composition ratio (x) of the prepared CdS_xSe_{1-x} was 0.66.

3.2. Crystalline structure

Fig. 2 presents the HXRD pattern of the CdS_xSe_{1-x} NWs with recorded diffraction peaks located at $2\theta = 24.60°$, 26.06°, and 27.91°, which corresponded to the (1 0 0), (0 0 2), and (1 0 1) planes, respectively, of the hexagonal structure. A comparison with the diffraction peaks listed in the standard data of XRD for the CdS compound (PDF-4-00-001-0780) showed that the position of the diffraction peaks in Fig. 2 is shifted toward low angles or toward the CdSe diffraction peak location (PDF-4-00-002-0330). This behavior suggests that NWs are composed of a solid solution of the CdS_xSe_{1-x} ternary alloy.

The lattice constants a and c for the hexagonal structure are calculated using the following equation [28]:

$$\frac{1}{d^2_{h\,k\,l}} = \frac{3}{4}\left(\frac{h^2+hk+k^2}{a^2}\right) + \frac{l^2}{c^2}, \quad (3)$$

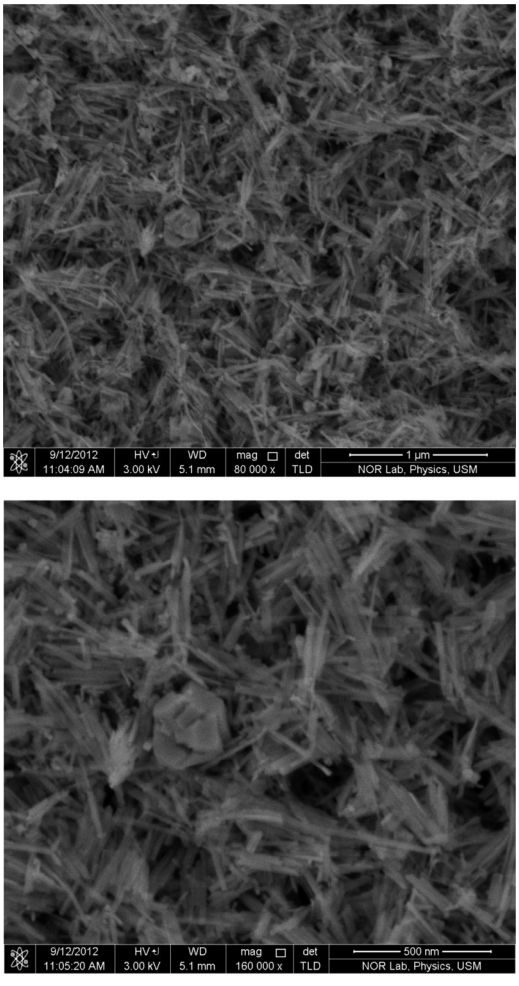

Fig. 1. SEM images of prepared CdS_xSe_{1-x} nanowires.

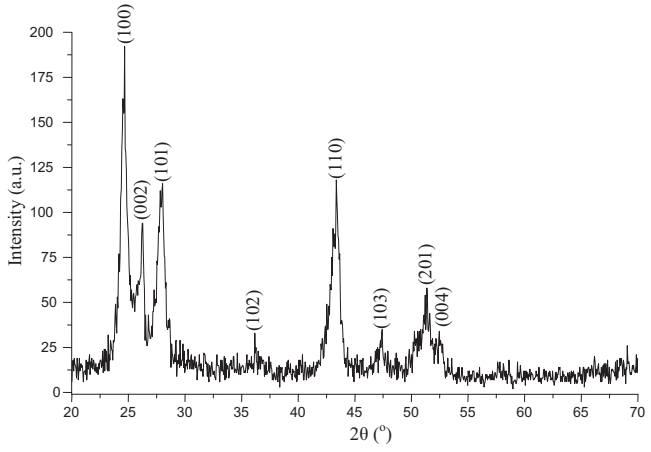

Fig. 2. XRD pattern of prepared CdS_xSe_{1-x} nanowires.

where d_{hkl} is the interplanar spacing of the atomic planes; and h, k, and l are the Miller indices.

The calculated values of the a and c parameters of $CdS_{0.66}Se_{0.34}$ NWs were 4.178 and 6.838 Å, respectively. The lattice-calculated values of the lattice parameters a and c were between the values of CdS (a = 4.142 Å, c = 6.724 Å) and CdSe (a = 4.30 Å, c = 7.02 Å), indicating that the CdS_xSe_{1-x} ternary alloy was formed. The relationship between the composition ratio (x) and the lattice parameters of the grown $CdS_{0.66}Se_{0.34}$ was found to obey an empirical formula as follows:

$$\begin{aligned} C_x &= 6.41 + 0.147x \\ a_x &= 4.137 + 0.165x \end{aligned}, \tag{4}$$

Yu et al. [29] prepared CdS_xSe_{1-x} NWs via solvothermal method with a composition ratio (x) range of 0–1 and concluded that low preparation temperatures (<180 °C) cannot provide enough activation energy to form the solid solution. They also noted that the samples synthesized at 180 °C for 12 h have a single hexagonal phase at x > 0.4 and x < 0.6, but two hexagonal phases, S rich or Se rich, were noted in the XRD patterns when x < 0.4 and x < 0.6. In our sample, the preparation temperature was 200 °C, and the x ratio was 0.66; thus, a single hexagonal phase is gated as shown in Fig. 2. The particle size (P_S) can be calculated from the peak broadening of HXRD by the Debye–Scherer's equation [30].

$$P_S = \frac{K \times \lambda}{\beta \cos\theta}, \tag{5}$$

where K is the shape factor, λ is the X-ray radiation wavelength (≈0.15 nm), β is the full half maximum (FWHM) of the HXRD diffraction peak, and θ is the half of the diffraction angle. The CdS NW growth direction was along ⟨0 0 1⟩; thus, the FWHM for the (0 0 2) plane was considered to calculate the P_S, and the estimated diameter (R_w) of the grown CdS NWs was $P_S = 2R_w$ [30]. The calculated P_S was approximately 15 nm.

3.3. Optical properties

3.3.1. Absorption of light

Fig. 3a shows the UV–vis absorption spectra of the $CdS_{0.66}Se_{0.34}$ NW. However, for direct band-gap materials, the optical energy gap was determined by extrapolating the straight-line segment of the $(\alpha h\nu)^n$ vs. $(h\nu)$ graphs to the $h\nu$-axis according to the following equation:

$$\alpha h\nu = A(h\nu - E_g)^n \tag{6}$$

where h is the Planck's constant, ν is the frequency, A is a constant that depends on the transition probability, E_g is the energy band gap, and the parameter n depends on the transmission type. Fig. 3b shows a plot of $(\alpha h\nu)^n$ as a function of $h\nu$ based on the assumption that n = 2. This finding indicates that the possible optical transition in the sample is direct and does not rely on phonons. The value of the optical band gap E_g was 2.38 eV for the $CdS_{0.66}Se_{0.34}$ NWs, whereas band gaps of 2.44 and 1.72 eV were estimated for the CdS and CdSe thin films, respectively [32]. The E_g values decreased with increasing Se content in the CdSSe alloy. However, the relationship between the optical band gap and composition ratio (x) in CdS_xSe_{1-x} alloy can be expressed by [32]:

$$E_g(x) = E_{CdSe}x + E_{CdS}x - 0.467x(1-x), \tag{7}$$

The x ratio was 0.66; thus, the E_g of the $CdS_{0.66}Se_{0.34}$ alloy was 2.084 eV. The obtained optical band gap was clearly higher than the value calculated from Eq. (6). In nanomaterials, two reasons could cause the increase in optical band gap: the quantum size effect and the very high surface-to-volume ratio. Khomane [33] found that the $CdS_{0.5}Se_{0.5}$ thin films prepared via chemical bath deposition have a direct optical band gap of 2.20 eV.

The crystallite size of the prepared $CdS_{0.66}Se_{0.34}$ NWs can also be determined using the effective mass model [34]:

$$E_g(\text{bulk}) = E_g(\text{nano}) + \frac{\hbar^2\pi^2}{2R^2}\left(\frac{1}{m_e^*} + \frac{1}{m_h^*}\right) - \frac{1.8e^2}{4\pi\varepsilon\varepsilon_o R} \tag{8}$$

where m_e^* and m_h^* are the effective masses of the electron in the conduction band (CB) and the hole in the valence band (VB), respectively, h is the Planck's constant, e is the electron charge, ε_o is the permittivity free space, ε is the relative permittivity, E_g is the energy gap of bulk CdS_xSe_{1-x}, and R or R_w is the particle radius. The electron and hole effective masses for the CdS_xSe_{1-x} ternary alloy were obtained from the bulk binary compound (CdS, CdSe) through linear interpolation [35].

The particle size ($P_S = 2R$ or R_w) value of the $CdS_{0.66}Se_{0.34}$ NWs was 5.2 nm. The obtained P_S is less than that calculated using the Debye–Scherer's equation. Mahdi et al. [34] discussed the reason for the difference of the P_S value from that calculated based on the XRD data and the effective mass model. They concluded that the total diffracted intensity for a given crystallite Bragg reflection is the sum of separately diffracted intensities by each unit-cell volume that creates the crystallite; big particles have higher electron densities than the small ones; thus, the diffracted intensity from the biggest particle is dominant.

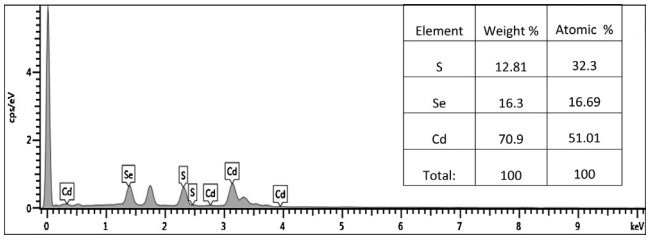

Fig. 3. EDX spectrum of prepared CdS_xSe_{1-x} nanowires.

3.3.2. Photoluminescence spectra

Cadmium chalcogenide bulk semiconductors possess high intrinsic PL quantum efficiency because of direct band transitions [5,36]. Fig. 4 shows the PL spectra of the prepared $CdS_{0.66}Se_{0.34}$ NWs. The PL spectra of the $CdS_{0.66}Se_{0.34}$ NWs showed a broad emission band located at 555 nm (2.23 eV). The obtained emission band was less than the calculated band gap of the prepared NWs, indicating that the electrons that exited to the CB flowed down to the defect level near the CB (0.15 eV below the CB) before the recombination process with the holes in the VB. The blue shift of the excitation emission band is commonly recognized to occur with decreasing crystallite size because of the quantum confinement effect in the nanostructures. No significant energy shift can be observed in the peak positions with the reduction in crystallite size. The presence of a PL peak at energy considerably lower than the band gap implies that the transition from the energy state in the band gap is attributed to the luminescence process in this nanostructured CdS_xSe_{1-x} NWs. Two broad emission bands were also detected at 826 (1.50 eV) and 880 nm (1.41 eV) wavelengths, which could be related to the recombination of a shallowly trapped carrier with the opposite carrier in a deep trap. Defect states almost appeared in the materials prepared via chemical methods because of low crystallinity. Pan et al. [32] noted disappearing defect emission bands in CdSSe NWs and nanoribbons that were prepared via thermal evaporation method using Au catalyst. They concluded that the prepared samples had high crystallinity, which led to disappearing defect states.

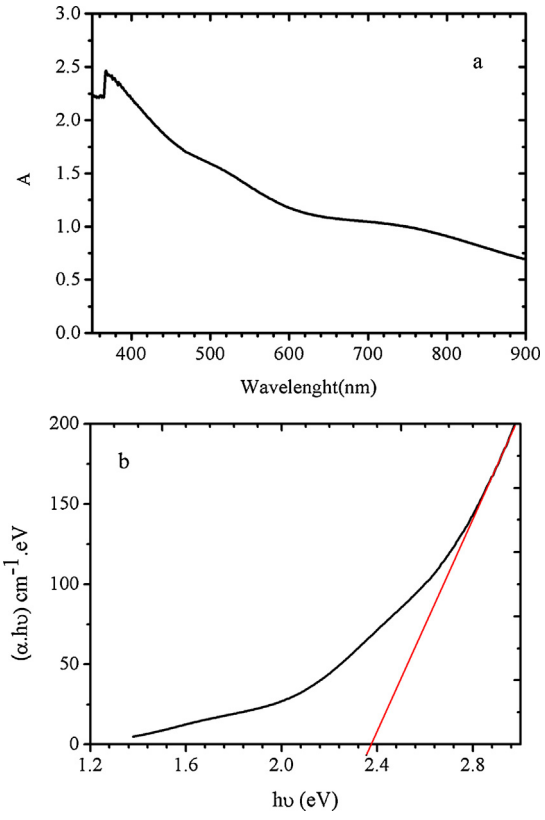

Fig. 4. (a) Absorption spectra of prepared CdS_xSe_{1-x} nanowires, (b) A plot of $(\alpha h\nu)^2$ vs $(h\nu)$ of prepared CdS_xSe_{1-x} nanowires.

3.3.3. *Raman shift*

Raman spectroscopy is a powerful tool for investigating the doping concentration, lattice defect identification, and crystal orientation of materials. The main features observed in the Raman scattering spectra of the II–VI nanocrystals were the longitudinal optical (LO) phonon mode (fundamental) and its overtones, which shifted to lower frequencies and broadened compared with the bulk crystal [37]. The Raman spectrum of the nanocrystalline CdS_xSe_{1-x} NWs is shown in Fig. 5. Two main broad peaks located at 285.51 and 908.49 cm^{-1} appeared in the Raman spectra, corresponding to the LO phonon and first overtone (2LO) of CdS_xSe_{1-x}, respectively. The LO peak locations in the bulk CdSe and CdS were 210 and 305 cm^{-1}, respectively [38]. Both blue- and red-shifts could be observed in the Raman spectra because of lattice contraction and quantum confinement, respectively [39]. Thus, Scamarico et al.

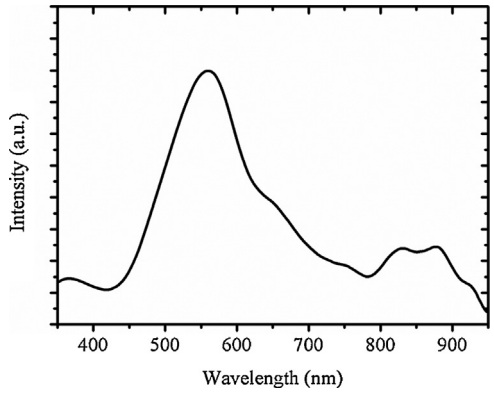

Fig. 5. Room temperature PL spectra of CdS_xSe_{1-x} nanowires prepared by solvothermal.

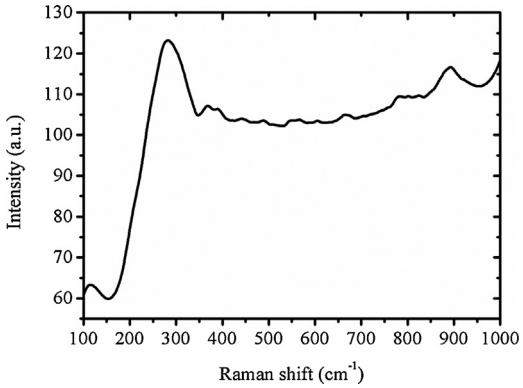

Fig. 6. Raman shift of CdS_xSe_{1-x} nanowires prepared by solvothermal.

[40] noted that the red-shift in the Raman spectra of CdS_xSe_{1-x} nanocrystals prepared with 5–20 nm diameter range is dominated (Fig. 6).

4. Conclusion

$CdS_{0.66}Se_{0.34}$ NW structure was successfully produced via solvothermal technique at 200 °C for 5 h. The FESEM images show that the grown wires had a uniform shape with a diameter range of 20–50 nm. The crystalline structure analysis of the prepared $CdS_{0.66}Se_{0.34}$ NWs showed that the NWs had a hexagonal phase. Interestingly, the crystallite size determined using XRD was 15 nm, whereas the size was 5.2 nm depending on the optical properties. In addition, the optical measurements revealed that the $CdS_{0.66}Se_{0.34}$ NW sample had a direct energy gap value of 2.38 eV. The PL spectra showed a main broad emission band located at 2.23 eV in addition to two other weak bands at 1.5 and 1.41 eV. The Raman spectra of the prepared $CdS_{0.66}Se_{0.34}$ NW sample showed the phonon confinement effect, where all the Raman peak positions of the LO and 2LO modes were 285.51 and 908.49 cm^{-1}, respectively.

Acknowledgments

The authors gratefully acknowledge the support of the FRGS (203/PFIZIK/6711353) grant and the Universiti Sains Malaysia.

References

[1] S. Park, H. Kim, C. Jin, C. Lee, Synthesis, structure, and photoluminescence properties of ZnSSe alloy nanorods, Curr. Appl. Phys. 12 (2012) 499–503.
[2] Y. Zou, D. Li, D. Yang, Single step synthesis of CdSeS nanorods with chemical composition gradients, J. Cryst. Growth 312 (2010) 3406–3409.
[3] H.F. Al-Taay, M.A. Mahdi, D. Parlevliet, Z. Hassan, P. Jennings, Preparation and characterization of silicon nanowires catalyzed by aluminum, Phys. E: Low-dimens. Syst. Nanostruct. 48 (2013) 21–28.
[4] Z.L. Wang, Characterizing the structure and properties of individual wire-like nanoentities, Adv. Mater. 12 (2000) 1295–1298.
[5] A.A. Ziabari, F.E. Ghodsi, Growth, characterization and studying of sol–gel derived CdS nanocrystalline thin films incorporated in polyethyleneglycol: effects of post-heat treatment, Sol. Energy Mater. Sol. Cells 105 (2012) 249–261.
[6] V. Kumara, A. Sharma, D.K. Sharma, D.K. Dwivedi, Effect of sintering aid ($CdCl_2$) on the optical and structural properties of CdZnS screen-printed film, Optik 125 (2014) 1209–1211.
[7] W.T. Yao, S.H. Yu, S.J. Liu, J.P. Chen, X.M. Liu, F.Q. Li, Architectural control syntheses of CdS and CdSe nanoflowers, branched nanowires, and nanotrees via a solvothermal approach in a mixed solution and their photocatalytic property, J. Phys. Chem. B 110 (2006) 11704–11710.
[8] S. Alam, M.A.K. Pathan, K.A.M.H. Siddiquee, A.B.M.O. Islama, M.A. Gafur, D.K. Saha, M. Mori, T. Tambo, Optical and structural characterization of CdSe and CdTe layers and fabrication of a CdTe/CdSe structure, Optik 124 (2013) 2165–2170.
[9] T.S. Shyju, S. Anandhi, R. Indirajith, R. Gopalakrishnan, Solvothermal synthesis, deposition and characterization of cadmium selenide (CdSe) thin films by thermal evaporation technique, J. Cryst. Growth 337 (2011) 38–45.

[10] A.S. Khomane, Structural and optical characterizations of chemically deposited cadmium selenide thin films, Mater. Res. Bull. 46 (2011) 1600–1603.
[11] I. Khan, I. Ahmad, H.A. Rahnamaye Aliabad, S.J. Asadabadi, Z. Ali, M. Maqbool, Conversion of optically isotropic to anisotropic CdS_xSe_{1-x} ($0 \le x \le 1$) alloy with S concentration, Comput. Mater. Sci. 77 (2013) 145–152.
[12] E.A. Sanchez-Ramirez, M.A. Hernandez-Perez, J. Aguilar-Hernandez, E. Rangel-Salinas, Nanocrystalline $CdS_{1-x}Se_x$ alloys as thin films prepared by chemical bath deposition: effect of x on the structural and optical properties, J. Alloys Compd. 615 (2015) S511–S514.
[13] A.A. Yadav, M.A. Barote, P.M. Dongre, E.U. Masumdar, Studies on growth and characterization of $CdS_{1-x}Se_x$ ($0.0 \le x \le 1.0$) alloy thin films by spray pyrolysis, J. Alloys Compd. 493 (2010) 179–185.
[14] Y.L. Kim, J.H. Jung, K.H. Kim, H.S. Yoon, M.S. Song, S.H. Bae, Y. Kim, The growth and optical properties of CdSSe nanosheets, Nanotechnology 20 (2009) 095605–095611.
[15] A.A. Yadav, E.U. Masumdar, Preparation and characterization of indium doped $CdS_{0.2}Se_{0.8}$ thin films by spray pyrolysis, Mater. Res. Bull. 45 (2010) 1455–1459.
[16] J.B. Chaudhari, N.G. Deshpande, Y.G. Gudage, A. Ghosh, V.B. Huse, R. Sharma, Studies on growth and characterization of ternary $CdS_{1-x}Se_x$ alloy thin films deposited by chemical bath deposition technique, Appl. Surf. Sci. 254 (2008) 6810–6816.
[17] G.S. Shahane, B.M. More, C.B. Rotti, L.P. Deshmukh, Studies on chemically deposited $CdS_{1-x}Se_x$ mixed thin films, Mater. Chem. Phys. 47 (1997) 263–267.
[18] D.S. Reddy, K. Narasimha Rao, K.R. Gunasekhar, Y.D. Reddy, P.S. Reddy, Synthesis and dc magnetic susceptibility of the diluted magnetic semiconducting $Cd_{1-x}Mn_xS$ nanocrystalline films, J. Alloys Compd. 461 (2008) 34–38.
[19] D.S. Reddy, K. Narasimha Rao, K.R. Gunasekhar, N.K. Reddy, K. Siva Kumar, P.S. Reddy, Annealing effect on structural and electrical properties of thermally evaporated $Cd_{1-x}Mn_xS$ nanocrystalline films, Mater. Res. Bull. 43 (2008) 3245–3251.
[20] M.M. El-Nahass, M.M. Sallam, M.A. Afifi, I.T. Zedan, Mater. Res. Bull. 42 (2007) 371.
[21] S. Augustine, S. Ampili, J. Ku Kang, E. Mathai, Structural, electrical and optical properties of Bi_2Se_3 and $Bi_2Se_{(3-x)}Te_x$ thin films, Mater. Res. Bull. 40 (2005) 1314–1325.
[22] Y. Liu, Y. Xu, J.P. Li, B. Zhang, D. Wu, Y.H. Sun, Synthesis of CdS_xSe_{1-x} nanorods via a solvothermal route, Mater. Res. Bull. 41 (2006) 99–109.
[23] K.P. Bhuvana, J. Elanchezhiyan, N. Gopalakrishnan, T. Balasubramanian, Optimization of $Zn_{1-x}Al_xO$ film for antireflection coating by RF sputtering, J. Alloys Compd. 473 (2009) 534–537.
[24] K. Sharma, A.S. Al-Kabbi, G.S.S. Saini, S.K. Tripathi, Thermally and optically induced effects on sub-band gap absorption in nanocrystalline CdSe (nc-CdSe) thin films, Curr. Appl. Phys. 13 (2013) 964–968.
[25] M.A. Mahdi, J.J. Hassan, S.S. Ng, Z. Hassan, Growth of CdS nanosheets and nanowires through the solvothermal method, J. Cryst. Growth 359 (2012) 43–48.
[26] S. Kar, S. Santra, H. Heinrich, Fabrication of high aspect ratio core–shell CdS–Mn/ZnS nanowires by a two step solvothermal process, J. Phys. Chem. C 112 (2008) 4036–4041.
[27] X. Wang, Y. Li, Solution-based synthetic strategies for 1-D nanostructures, Inorg. Chem. 45 (2006) 7522–7534.
[28] B.D. Cullity, Elements of X-ray diffraction, Addison-Wesley, Reading, USA, 1972.
[29] S.H. Yu, J. Yang, Z.H. Han, R.Y. Yang, Y.T. Qian, Y.H. Zhang, Novel solvothermal fabrication of CdS_xSe_{1-x} nanowires, J. Solid State Chem. 147 (1999) 637–640.
[30] M.A. Mahdi, J.J. Hassan, S.J. Kasim, S.S. Ng, Z. Hassan, Solvothermal growth of single-crystal CdS nanowires, Bull. Mater. Sci. 37 (2014) 337–345.
[32] A. Pan, H. Yang, R. Yu, B. Zou, Fabrication and photoluminescence of high-quality ternary CdSSe nanowires and nanoribbons, Nanotechnology 17 (2006) 1083–1086.
[33] A.S. Khomane, Crystallographic and microscopic properties of ternary $CdS_{0.5}Se_{0.5}$ thin films, Optik 124 (2013) 2432–2435.
[34] M.A. Mahdi, Z. Hassan, S.S. Ng, J.J. Hassan, S.K.M. Bakhor, Structural and optical properties of nanocrystalline CdS thin films prepared using microwave-assisted chemical bath deposition, Thin Solid Films 520 (2012) 3477–3484.
[35] S. Adachi, Properties of Semiconductor Alloys: Group-IV, III–V and II–VI Semiconductors, John Wiley & Sons Ltd, UK, 2009.
[36] P.Y. Yu, M. Cardona, Fundamentals of Semiconductors, Springer-Verlag, 2001.
[37] V. Dzhagan, M. Valakh, N. Mel'nik, O. Rayevska, I. Lokteva, J.K. Olestrich, D.R.T. Zahan, Phonon spectra of small colloidal II–VI semiconductor nanocrystals, Int. J. Spectrosc. ID 532385 (2012) 6.
[38] V.M. Dzhanan, M.Y. Valakh, A.E. Raevskaya, A.L. Stroyuk, S.Y. Kuchmiy, D.R.T. Zahn, Nanotechnology 18 (2007) 78501–785017.
[39] R. Venugopal, P. Lin, C.C. Liu, Y.T. Chen, Surface-enhanced raman scattering and polarized photoluminescence from catalytically grown CdSe nanobelts and sheets, J. Am. Chem. Soc. 127 (2005) 11262–11268.
[40] G. Scamarico, M. Lugara, D. Manno, Size-dependent lattice contraction in nanocrystals embedded in glass observed by Raman scattering, Phys. Rev. B 45 (1992) 13792–13795.